Eco-Mechanical Performances of Reinforced Concrete

A.P. Fantilli[1], B. Chiaia[2]

ABSTRACT: A new eco-mechanical index (EMI) has been introduced with the aim of quantifying the environmental impact of concrete structures. From a general point of view, this indicator represents the amount of carbon dioxide released to produce certain mixtures of pre-established strength and ductility. Both for normal strength and high strength concrete, with and without steel fibers, these mechanical properties are summarized by the work of fracture under tensile actions. If also structural durability has to be taken into account, the maximum crack width of reinforced concrete structures must be computed. This is possible by using a tension-stiffening model, here applied to reinforced concrete elements in tension. However, with or without the evaluation of crack width, the concrete with the best EMI releases the highest fracture energy. For this reason, the work of fracture represents also a durability parameter, and therefore it can be used to tailor cement-based composites with the highest strength, ductility, and durability, and the lowest environmental impact.

1 INTRODUCTION

The production of cement and cement-based composites, like structural concrete, is not an environmental friendly process. Evaluating the environmental stress produced by concrete structures during the different phases of life is therefore a basic design requirement (fib 2010). This is possible by estimating either the global energy consumed or, equivalently, the CO_2 footprint calculated through the entire cycle of life.

According to Ashby (2009), in the case of concrete structures, 90% of total life-energy is necessary to create the material (i.e., mostly clinker), whereas only 10% is related to product manufacturing, transportation and use. For these reasons, in order to increase the eco-efficiency of concrete constructions, new mix-design procedures aiming at reducing CO_2 emission need to be introduced. For instance, it is possible to select the components that show very favorable values of the so-called sustainability reporting instruments, which focus on sustainable development indicators, or green labels based on life cycle assessment (Blengini & Shields, 2010). However, such instruments are used without considering the structural behavior of the final product. To be more precise, the evaluation of CO_2 released by concrete production is the unique motivation for these analyses, which completely disregard the mechanical performances of materials, quite surprisingly, as concrete is a structural material.

Conversely, the two strategies suggested by Habert & Roussel (2009) are more effective than the sustainability reporting instruments for reaching carbon mitigation targets, even if they are not completely satisfactory. Indeed, the first strategy, generally called material performance strategy, is based on the reduction of clinker by reducing the total amount of concrete, and thus the volume of structures. Obviously, the mechanical per-

[1] *Assistant Professor, Politecnico di Torino, alessandro.fantilli@polito.it*
[2] *Professor,Politecnico di Torino, bernardino.chiaia@polito.it*

formances, such as the compressive strength f_c, need to be increased with respect to classical concrete under the same loading demand. It has been estimated that the CO_2 released by the construction of concrete columns can be reduced of about 20%, when f_c increases from 40 MPa to 60 MPa (Habert & Roussel 2009). Nevertheless, the cost of such enhancement of strength is not always competitive, and frequently high strength concrete can show very brittle behavior, especially under compression (Li & Park 2004). Slenderness and instability represent another drawback.

The last strategy consists in substituting clinker with cementitious and/or pozzolanic mineral admixtures, such as fly ashes and silica fumes (Mehta & Monteiro 2006). However, this strategy can be very expensive and the final properties of concrete are often not enhanced, particularly in the case of poor quality ingredients or poor mixture proportioning.

To obtain the optimum mixture, concrete components should be selected by means of approaches capable of exploiting and optimizing both the eco-efficiency and the structural performances of cement-based composites (Swamy 2007). In other words, according to Rilem TC 172 (1999), the environmental aspects must be put into a set of other design aspects. Damineli et al. (2010), for instance, introduced the CO_2 intensity indicator and the binder intensity index, which represent, respectively, the total emitted carbon dioxide and the amount of binder necessary to deliver 1 MPa of strength. However, in both cases only the compressive strength of concrete is considered, whereas tensile strength and post-peak energy absorption (i.e., the ductility) are neglected. The latter mechanical property, which can also be related to cracking and permeability, is of fundamental importance to assess concrete durability (Picandet, 2001).

Thus, new and more appropriate indicators need to be introduced in order to reduce the CO_2 emission and maintain, or increase, strength, ductility and durability of concrete.

2 NOGHABAI'S TESTS ON CONCRETE UNDER TENSION

Noghabai (1998) tailored several high strength and normal strength concretes, with and without fiber-reinforcement. Among all the tests, the following mixtures are herein considered:

- NSC: plain normal strength concrete.
- NSCs: normal strength concrete reinforced with two types of steel fibers (0.5% in volume of long fibers – diameter 0.6 mm and length 30 mm –, and 0.5% in volume of short fibers – diameter 0.15 mm and length 6 mm).
- HSC: plain high strength concrete.
- HSCs: high strength concrete reinforced with two types of steel fibres (0.5% in volume of long fibers – diameter 0.6 mm and length 30 mm –, and 0.5% in volume of short fibers – diameter 0.15 mm and length 6 mm).

As Fig.1a shows, all the above mixtures are subjected to uniaxial tensile loads, applied to notched cylinders, having a height equal to 85 mm and a diameter of about 70 mm.

As a result, the post-peak stress (σ_c) – crack opening displacement (w) curves are obtained. Such curves, normalized with respect to the tensile strength f_{ct} and limited to the maximum crack width $w_c = 3$ mm, are depicted in Fig.1b.

The area A_F delimited by the σ_c/f_{ct}-w curves is due to the fracture process. If this area is multiplied by the strength f_{ct}, the work of fracture G_F can be obtained. In the case of the concretes mixtures investigated in the present work, the values of G_F, together with the elastic modulus E_c and the compressive strength f_c, are reported in Table 1.

The softening branch of NSC does not show tensile stresses when crack widths are larger than 0.3 mm. A similar behavior can be observed also in the case of HSC without steel fibers. Indeed, the $\sigma_c / f_{ct} - w$ curves (and consequently the values of A_F) are nearly the same in both concretes (Fig.1b). However, due to the lower tensile strength of NSC, the work of fracture G_F is larger in HSC.

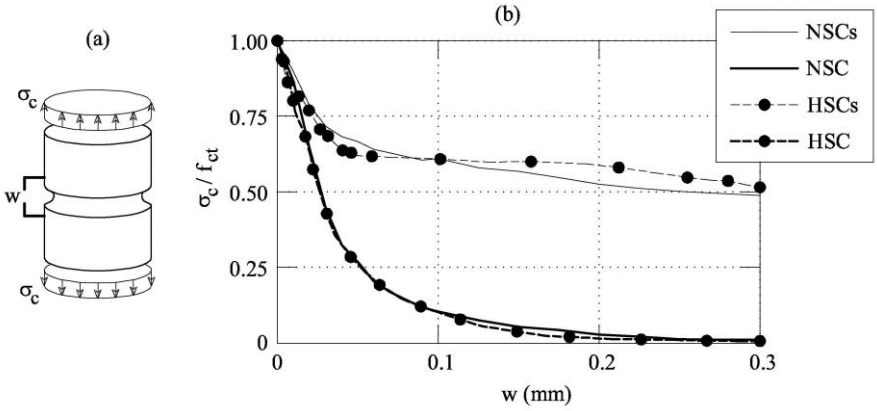

Figure 1. Uniaxial tensile tests performed by Noghabai (1998): (a) notched specimen; (b) normalised stress vs. crack opening displacement curves.

Conversely, both NSCs and HSCs show a very ductile response, because of the fiber-reinforcement. The normalized post-peak branches, and the values of A_F as well, are similar. Nevertheless, a higher fracture work is released by HSCs.
Table 1 also shows the amount of cement and the global fiber volume fraction used to cast the concretes.

Table 1. Mechanical properties of the Noghabai's (1998) concretes.

Specimen	Cement	Fiber	f_{ct}	f_c	G_F	A_F	E_c
	(kg/m^3)	(%)	(MPa)	(MPa)	(N/mm)	(mm)	(GPa)
NSC	350	0	3.7	65.1	0.17	0.05	37.2
NSC_S	350	1	4.1	55.9	0.73	0.18	32.2
HSC	490	0	5.1	122	0.21	0.05	41.5
HSCs	490	1	5.75	127	1.05	0.18	36.5

3 MODELLING THE CRACKING PHENOMENON OF RC TIES

The RC members in tension depicted in Fig.2 can be considered a reasonable prototype to analyze all the phenomena involved in the cracking of RC structures. According to Fantilli et al. (1998), in these structures the crack pattern cannot be univocally defined.
As soon as the applied normal force N reaches the cracking load N_{cr}, cracks can take place in any of the cross-sections of the zone L-$2l_{tr}$ (L = global length of the tie) where concrete stresses σ_c equate the tensile strength f_{ct}.

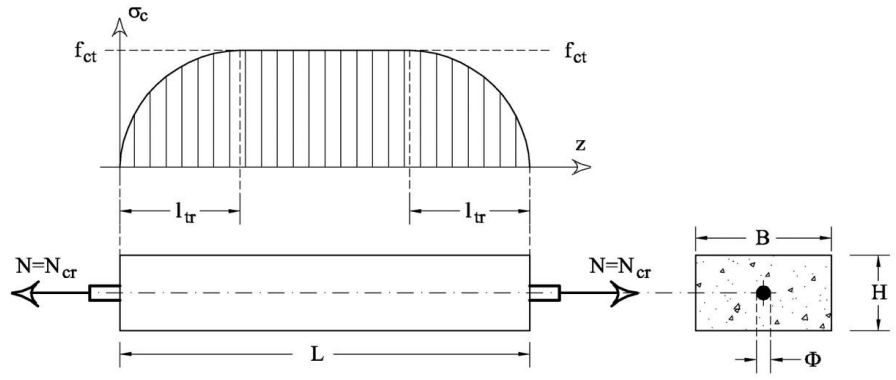

Figure 2. Tensile stresses in the concrete surrounding a steel reinforcing bar in tension.

3.1 Formulation of the Problem

The random nature of cracking leads to the analysis of tie's blocks delimited by two consecutive cracked cross-sections (i.e., the Type 1 cross-section depicted in Fig.3a), whose states of strain and stress are illustrated in Fig.3b and Fig.3c, respectively. For given axial load *N*, concrete strains (ε_c) and steel strains (ε_s) (and the related stresses σ_c and σ_s) can be obtained through the following equilibrium equation (Fig.3a):

$$N = \sigma_s A_s + \sigma_c A_c = E_s \varepsilon_s A_s + E_c \varepsilon_c A_c \tag{1}$$

where, A_s = area of steel rebars in tension; A_c = area of concrete; E_c = Young's modulus of concrete; and E_s = Young's modulus of steel. According to Eq.(1), the structural analysis is here performed within the serviceability stage of RC structures, where steel and uncracked concrete behave in a linear elastic manner.

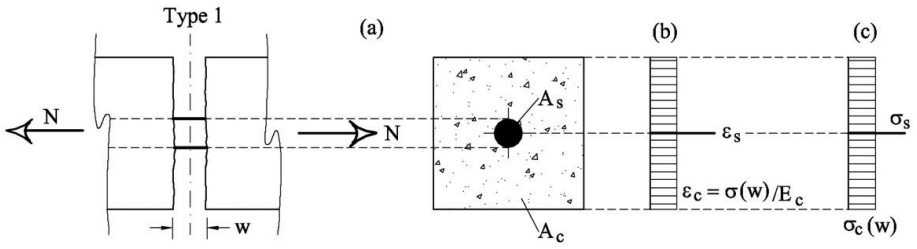

Figure 3. RC ties: (a) Geometrical properties of Type 1 cross-section; (b) State of strain; (c) State of stress.

In a RC tie, the maximum value of the crack width *w*, assumed to be constant in the cracked cross-section under the load *N*, is reached at the incipient formation of a new crack. At the same time, the maximum crack spacing (i.e., 2 l_{tr}), which is the distance between two existing cracks, is halved as the new crack growths (Fantilli et al. 1998).
The incipient formation of a new crack is schematized in Fig.4, where Type 2 cross-section shows the maximum tensile stress in concrete (i.e., $\sigma_c = f_{ct}$ in Fig.4c). In the same cross-section, steel strains (Fig.4b) and steel stresses (Fig.4c) can be computed by means of Eq.(1).

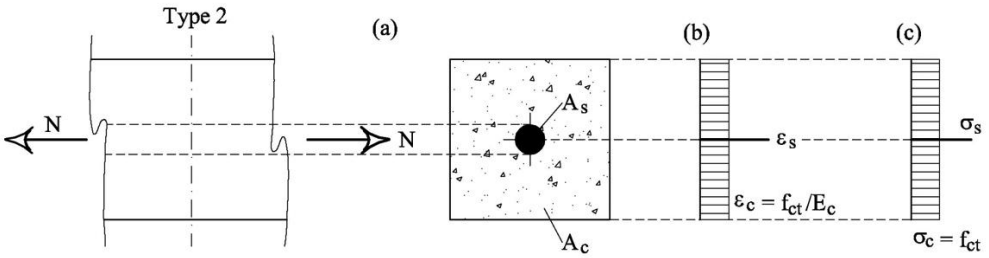

Figure 4. RC ties: (a) Geometrical properties of Type 2 cross-section; (b) State of strain; (c) State of stress.

In each portion of the tie, the interaction between steel and concrete can be described by the classical equilibrium and compatibility equations:

$$\frac{\partial \sigma_s}{\partial z} = -\frac{4}{\Phi} \cdot \tau \tag{2}$$

$$\frac{\partial s}{\partial z} = -\varepsilon_s + \varepsilon_c \tag{3}$$

where, Φ = diameter of the steel reinforcing bar; s = value of slip between rebar and concrete; z = horizontal coordinate; and τ = bond stress acting at the steel-concrete interface. To complete the formulation of the problem, the fictitious crack model of concrete in tension and the bond-slip relationship τ-s have to be defined. The curves depicted in Fig.1b, and the values reported in Table 1, define the σ-w relationships used to model the nonlinear behavior of cracked concrete. Conversely, in absence of splitting failures, the τ-s relationship proposed by Model Code (fib 2010) and reported in Fig.5, is used in the case of plain concrete. This relationship is similar to that proposed by Harajli et al. (1995) for FRC, although the main parameters (i.e. the bond strength τ_{max} and the slip at peak s_1) assume different values (Fig.5).

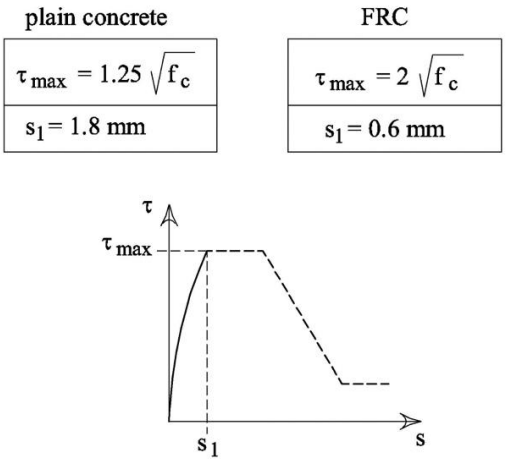

Figure 5. Bond-slip relationships for plain (fib, 2010) and fiber-reinforced concrete (Harajli 1995).

3.2 Numerical solution

Type 1 (Fig.3) and Type 2 (Fig.4) cross-sections limit the block of length l_{tr} (Fig.6) herein used to model tension-stiffening in RC structures. In particular, such a tie's portion is the domain where Eqs.(2)-(3) have to be integrated under to the following boundary conditions:

- $s(z = 0) = w/2$ (in Type 1 cross-section, where $z = 0$);
- σ_c $(z = l_{tr}) = f_{ct}$ (in Type 2 cross-section, where $z = l_{tr}$).

Moreover, due to the symmetry, in the Type 2 cross-section the condition s =0 should also be verified.

This problem can be numerically solved by the following iterative procedure:

1. Assume a value for the crack width w in Type 1 cross-section (Fig.6a).
2. Assume a trial value for the tensile strain of rebar in Type 1 cross-section (Fig.6c).
3. From the equilibrium of the Type 1 cross-section [Eq.(1)] the normal force N can be calculated.
4. From the equilibrium of the Type 2 cross-section [Eq.(1)], it is possible to obtain the steel strains (and stresses) in the cross-section at incipient cracking.
5. Assume a trial value for the length l_{tr} of the block depicted in Fig.6, and divide the transfer length into n part parts of length $\Delta z = l_{tr}/n$.
6. As the static and kinematic conditions are known at the borders of the tie's portion, Eqs.(2)-(3) can be numerically integrated. In a generic i-th point of the domain, the increments of concrete strains (Fig.6b) are assumed to be similar to the decrements of steel strains (Fig.6c), according to the following formulae:

$$\varepsilon_{s,i} = \varepsilon_{s,0} - \chi_i \left(\varepsilon_{s,0} - \varepsilon_{s,n} \right) \tag{4}$$

$$\varepsilon_{c,i} = \varepsilon_{c,0} - \chi_i \left(\varepsilon_{c,0} - \varepsilon_{c,n} \right) \tag{5}$$

where, $\varepsilon_{c,n}$ and $\varepsilon_{s,n}$ = strain in concrete and steel, respectively, in Type 2 cross-section; $\varepsilon_{c,0}$ and $\varepsilon_{s,0}$ = strain in concrete and steel, respectively, in Type 1 cross-section; χ_i = coefficient of similarity ($0 \le \chi_I \le 1$). By applying the explicit finite difference method to Eq.(3), and by substituting Eqs.(4-5), it is possible to define s_i as a function of χ_i (Fig.6d):

$$s_i = s_{i-1} - \Delta z \left[-\chi_i \left(\varepsilon_{s,0} - \varepsilon_{s,n} - \varepsilon_{c,0} + \varepsilon_{c,n} \right) + \varepsilon_{s,0} - \varepsilon_{c,0} \right] \tag{6}$$

Similarly, if the explicit finite difference method is applied to Eq.(2), it is possible to compute the steel strain $\varepsilon_{s,i}$ through the equation (Fig.6c):

$$\varepsilon_{s,i} = \varepsilon_{s,i-1} - \Delta z \frac{4}{\Phi E_s} \tau_{i-1} \tag{7}$$

Moving from the left border (cracked cross-section in Fig.6a) to the right border (point n in Fig.6a), Eqs.(4)-(7) provide the values of $\varepsilon_{s,i}$ – Eq.(7) –, χ_i – Eq.(4) –, $\varepsilon_{c,i}$ – Eq.(5) –, and s_i – Eq.(6) .

7. If at n^{th} point $s_n \neq 0$ (Fig.6d), change l_{tr} and go back to step 6.

8. If at n^{th} point $\varepsilon_{c,n} \neq f_{ct}/E_c$ (and therefore $\chi_i \neq 1$), change $\varepsilon_{s,0}$ and go back to step 2.
For a given value of crack width *w*, the previous procedure provides not only the corresponding normal force *N*, but also the maximum distance between the cracks $s_{r,max} = 2\, l_{tr}$.

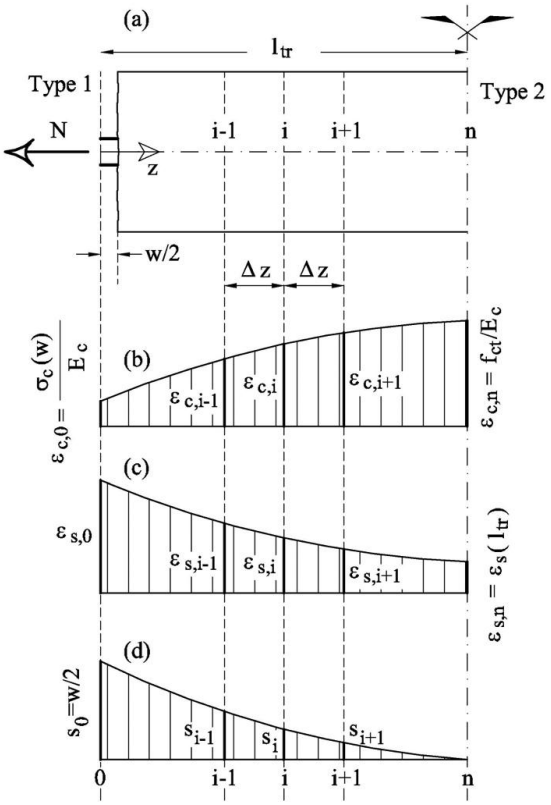

Figure 6. The portion of a RC tie used to model the tension stiffening.

3.3 Application of the Model

The proposed model can be used to predict the crack pattern, both in terms of crack spacing and crack width, in RC elements under tensile loads (Fig.2). Specifically, the specimen tested by Mitchell et al. (1996) is firstly investigated.
The evolution of the maximum crack width, experimentally measured at different values of applied load N, is depicted in Fig.7. In the same Figure, the curve computed with the proposed numerical procedure is also reported. The good agreement between the experimental data and the theoretical results demonstrates the capability of the proposed approach to predict effectively the cracking process of RC ties.
Fig.8b shows the crack widths predicted in the case of the RC ties depicted in Fig.8a and made with the four concretes tested by Noghabai (1998). Fibers can reduce crack width, under a given external load N. This aspect can be observed in both HSC and NSC ties, even if the latter can show a wider crack opening with and without fibers.

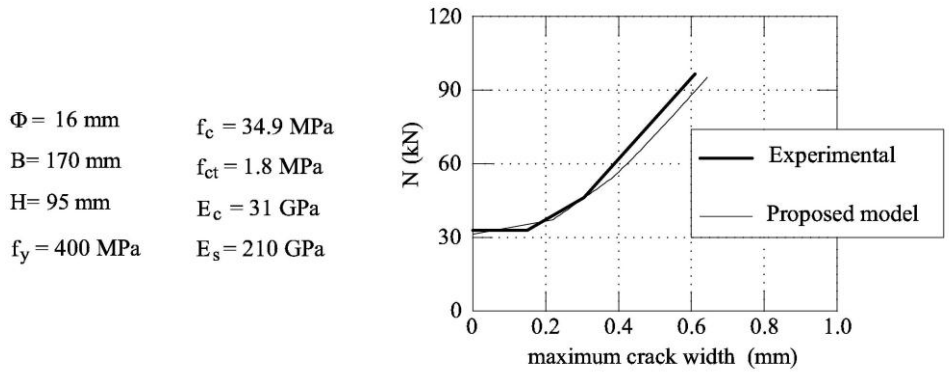

Figure 7. Comparison between the maximum crack width predicted by the proposed model and the values measured by Mitchell et al. (1996).

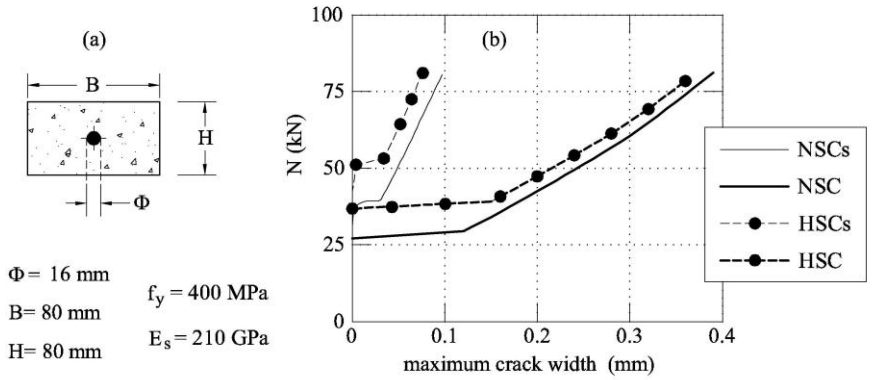

Figure 8. Application of the proposed tension stiffening model: (a) geometry of the RC ties; (b) predicted crack width.

4 ECO-MECHANICAL PERFORMANCE OF RC MEMBERS IN TENSION

With the aim of selecting the concrete with the best mechanical properties and the lowest environmental impact, a new procedure is here introduced. Ecological performances are quantified by the amount of CO_2 released by the production of cement and fibers used to cast the concrete (the carbon footprint of the other components is not considered). Conversely, the mechanical performances can be related to the serviceability state of concrete structures.

According to Swamy (2007), the best concrete has to be selected through a holistic approach, capable of integrating the environmental footprint and the mechanical performances. It is based on some eco-mechanical indexes (*EMI*), in which the CO_2 pollution represents the denominator, whereas the mechanical properties are at the numerator:

$$EMI = \frac{mechanical\ properties}{CO_2\ released} \tag{8}$$

From a general point of view, the best eco-mechanical performances are reached when the *EMI*, related to certain mixtures available on the construction market, is the highest. In the serviceability stage, f_{ct} (i.e., strength) and A_F (i.e., ductility) are the mechanical

performances that need to be maximized. In other word, the work of fracture G_F can be introduced in the numerator of Eq.(8):

$$EMI_1 = \frac{G_F}{Q_{cc} + Q_{cf}} \tag{9}$$

where, Q_{cc} = amount of carbon dioxide (measured in kg) necessary to produce the cement used to cast a cubic meter of concrete; Q_{cf} = amount of carbon dioxide (measured in kg) necessary to produce the steel fibers added to the unit volume (m^3) of concrete. These quantities can be easily estimated when the constituents of concrete are known. Specifically, according to the Ecoinvent database developed by Swiss Centre for Life Cycle Inventories (2012), 0.83 kg and 1.79 kg of CO_2 are released for the production of 1 kg of Portland cement and 1 kg of low carbon steel, respectively.
Nevertheless, for a given value of load N applied to the specimens depicted in Fig.8a, the value of the maximum crack width w_{max} has to be minimized (fib 2010). Thus, in a more complete formulation of *EMI*, the parameter G_F/w_{max} should be introduced in the case of RC structures:

$$EMI_2 = \frac{G_F / w_{max}}{Q_{cc} + Q_{cf}} \tag{10}$$

The average values of EMI_1 are reported in the histogram of Fig.9a. Fig.9b shows the eco-mechanical performances when also durability (i.e., EMI_2) is taken into account.

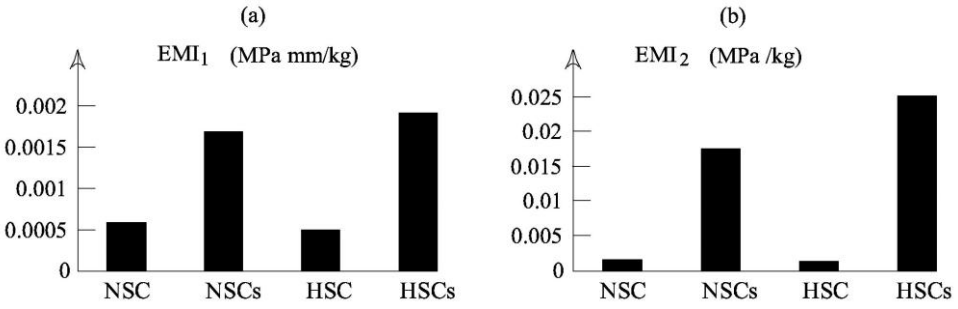

Figure 9. Eco-Mechanical Index: (a) values of EMI1 ; (b) values of EMI2.

Although the numerical values of EMI_1 and EMI_2 are different, the comparative analysis of the concrete mixtures under investigation gives the same result. From an eco-mechanical point of view, fiber-reinforced composites (i.e., NSCs and HSCs) behave better than plain NSC and HSC. However, when the same amount of steel fibers is used (0% or 1% in volume), EMI_1 and EMI_2 are higher for HSC. Thus, without computing w_{max}, the work of fracture G_F can be also used to characterize the durability performance of RC structures.

5 CONCLUSIONS

From the results of a numerical analysis, performed on different types of reinforced concrete ties, the following conclusions can be drawn:

- HSC behaves better than NSC, not only in terms of strength but also in terms of reduced crack width.

- In a sustainability analysis of concrete structures, the work of fracture G_F is itself sufficient to define mechanical and durability performances of NSC and HSC, with and without fiber-reinforcement.
- Eq.(9) is the best way for tailoring cement-based composites with the highest strength, ductility and durability, and with the lowest environmental impact.

The present eco-mechanical approach is only based on the fracture work in tension (i.e., G_F), which can be measured by means of complex test setups. Thus, further researches should be developed in order to use only the fracture toughness measured in compression tests.

REFERENCES

Ashby, M.F. (2009). *Materials and the Environment: Eco-informed Materials Choice*, Butterworth-Heinemann (Elsevier), London.

Blengini, G.A., Shields, D.J. (2010). "Green labels and sustainability reporting - Overview of the building products supply chain in Italy", *Management of Environmental Quality: An International J.*, 21, 477-493.

Damineli, B.L., Kemeid, F.M., Aguiar, P.S., John, V.M. (2010). "Measuring the eco-efficiency of cement use", *Cement and Concrete Composites*, 32, 555–562.

Fantilli, A.P., Ferretti, D., Iori, I., Vallini, P. (1988). "Flexural Deformability of Reinforced Concrete Beams", *ASCE Journal of Structural Engineering*, 124(9), 1041-1049.

fib. (2010). *Model Code 2010 - First complete draft*. fib Bulletin 55.

Habert, G., Roussel, N. (2009). "Study of two concrete mix-design strategies to reach carbon mitigation objectives", *Cement and Concrete Composites*, 31, 397–402.

Harajli, M.H., Hout, M., Jalkh, W. (1995). "Local Bond Stress-Slip Relationship of Reinforcing Bars Embedded in Plain and Fiber Concrete", *ACI Materials Journal*, 92(4), 343 - 354.

Li, B., Park, R. (2004). "Confining Reinforcement for High-Strength Concrete Columns", *ACI Structural Journal*, 101, 314-324.

Mehta, P.K., Monteiro, P.J.M. (2006). *Concrete - Microstructure, Properties, and Materials*. McGraw-Hill, New York.

Mitchell D., Abrishami H.H., Mindess S. (1996). "The Effect of Steel Fibers and Epoxy-Coated Reinforcement on Tension Stiffening and Cracking of Reinforced Concrete", *ACI Materials Journal*, 93(1), 61-68.

Noghabai, K. (1998). *Effect of tension softening on the performance of concrete structures*. Doctoral thesis, Luleå University of Technology, 21.

Picandet, V., Khelidj, A., Bastian, G. (2001). "Effect of axial compressive damage on gas permeability of ordinary and high-performance concrete", *Cement and Concrete Research*, 31, 1525-1532.

Rilem TC 172 (1999). "Environmental design methods in materials and structural engineering —Progress Report of RILEM TC 172-EDM/CIB TG 22", *Materials and Structures*, 32, 699-707.

Swamy, R.N. (2007). Design for sustainable development of concrete construction. In *Proceedings of the Fourth International Structural Engineering and Construction Conference (ISEC 4)*, Taylor & Francis Ltd, England, 47-54.

Swiss Centre for Life Cycle Inventories (2012). "Ecoinvent Centre". <http://www.ecoinvent.ch> (accessed June 2013).